

Short Note

Amplitude behavior in angle gathers

*Carmen B. Mora*¹

INTRODUCTION

In a previous report, Sava and Fomel (2000) presented a method for computing angle-domain common-image gathers by a radial-trace transform in the Fourier domain. The method converts offset-domain common-image gathers, which are computed using 2-D prestack wave-equation migration (Prucha et al., 1999) into true reflection angle-domain common-image gathers.

Obtaining the output images in angle-domain is very attractive for amplitude versus angle (AVA) analysis. However, because the application of AVA analysis is to detect anomalous amplitude behavior, we need to understand how the relative amplitudes are affected by the method in order to guarantee that the method itself is not a source of amplitude distortions.

According to the AVA analysis theory, the variation of seismic reflection coefficients with angle (and offset) can be used as a direct hydrocarbon indicator (Ostrander, 1984; Swan, 1993). The physical relationship between the variation of reflection/transmission coefficients with incident angle and rock parameters has been widely investigated. This relationship is established in the Zoeppritz equations (Mavko et al., 1998), which relate reflection and transmission coefficients for plane waves and elastic properties of the medium.

In this note, I investigate the amplitude behavior of angle gathers using two synthetic data sets. I compare the resulting amplitudes from angle-domain common-image gathers with the amplitudes from offset-ray parameter images obtained using two different approaches: prestack wave-equation migration (Prucha et al., 1999) and migration/inversion (Prucha et al., 2000).

SYNTHETIC DATA

I generated two synthetic data sets assuming an earth model that includes two flat layers with constant elastic properties on each layer. In model 1, I chose the same elastic properties for both the overlaying and the underlying layer, which results in no AVA effect along the

¹**email:** cmora@sep.stanford.edu

interface. In model 2, I chose rock properties corresponding to velocity and density contrast in the underlying layer which leads to an AVA effect of decreasing amplitudes with increasing angle on incidence. Figure 1 shows the expected P -wave reflection coefficient corresponding to model 1 and model 2, calculated using Zoeppritz equations.

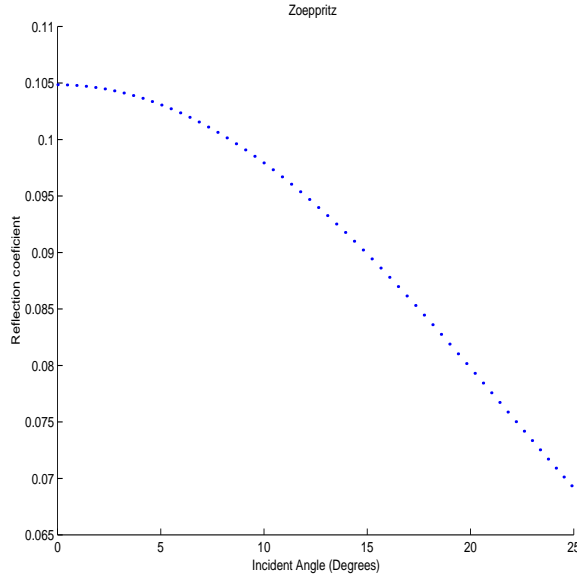


Figure 1: P -wave reflection coefficient from Zoeppritz equations for model 1 (left) and model 2 (right). cmora1-Zoeppritz [CR]

The modeling was done using a ray tracing approach to get the timing of the event and using the exact Zoeppritz equations to set the amplitude values. Figure 2 shows the picked amplitudes for the resulting modeled data.

PROCESSING

I applied three different processing sequences to each data set in order to compare the resulting amplitudes from angle-domain common-image gathers with the amplitudes from offset-ray parameter images.

1. Prestack wave-equation migration with output in offset domain + conversion to angle gather by Fourier transform.
2. Prestack wave-equation migration with output in offset ray parameter domain.
3. Iterative execution of prestack wave-equation migration and inversion with output in offset ray parameter domain (10 iterations).

Figure 3 shows the resulting CIG gathers for each processing sequence in model 1 and Figure 4 shows the resulting CIG gathers in model 2. We can see some artifacts that are stronger

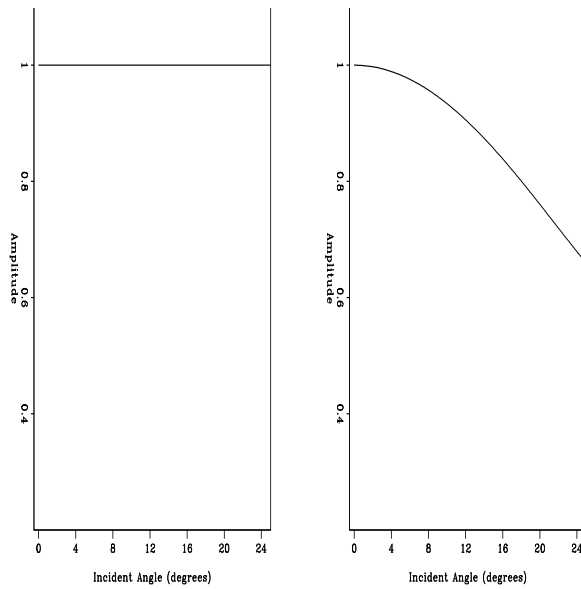


Figure 2: Picked amplitudes at the flat reflector for the resulting modeled data for model 1 (left) and model 2 (right). `cmora1-avo_data` [CR]

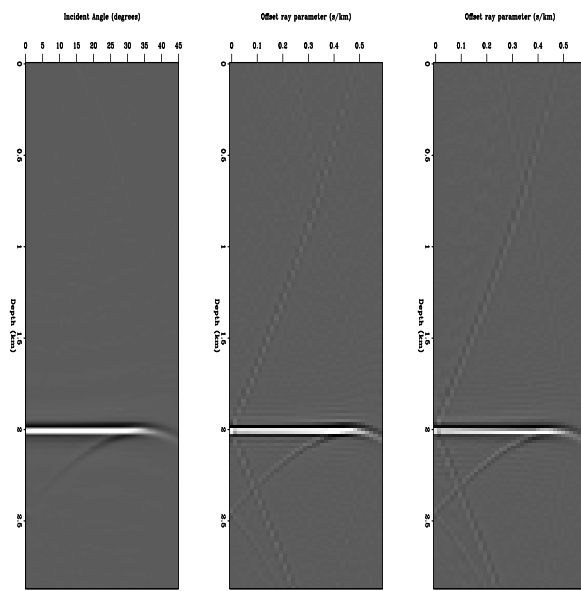


Figure 3: CIG result of applying the 3 processing sequences to model 1. Left: Prestack wave-equation migration with output in offset domain + conversion to angle gather by Fourier transform. Middle: Prestack wave-equation migration with output in offset ray parameter domain. Right: Iterative execution of prestack wave-equation migration and inversion with output in offset ray parameter domain. `cmora1-image-con-all` [CR]

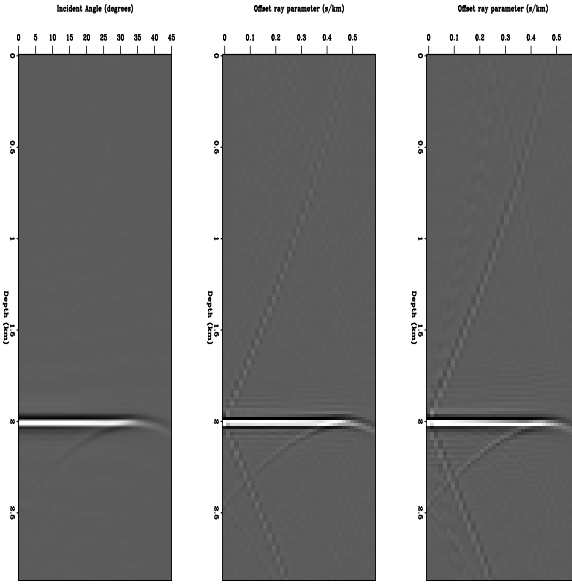


Figure 4: CIG result of applying the 3 processing sequences to model 2. Left: Prestack wave-equation migration with output in offset domain + conversion to angle gather by Fourier transform. Middle: Prestack wave-equation migration with output in offset ray parameter domain. Right: Iterative execution of prestack wave-equation migration and inversion with output in offset ray parameter domain. cmora1-image-avo-all [CR]

in cases 2 and 3. These artifacts could affect the amplitudes values in the near and far offset. Also, for cases 2 and 3, the output is in the offset ray parameter domain which is not directly the angle of incidence; the offset ray parameter, p_{hx} , is related to the aperture angle θ , the dip ϕ along the in-line direction, and the velocity function $V(z, \mathbf{m})$, as follows (Prucha et al., 1999):

$$p_{hx} = \frac{2 \sin \theta \cos \phi}{V(z, \mathbf{m})} \quad (1)$$

Therefore, for cases 2 and 3, I calculated the conversion to the angle domain using the relation from equation (1). Figure 5 shows the picked amplitudes at the flat interface in the migrated CIG gather for model 1. Figure 6 shows the picked amplitudes at the flat interface in the migrated CIG gather for model 2.

DISCUSSION

From Figures 5 and 6 we can observe that, in general, results from angle gather are smoother and have a shape more similar to the theoretical tendency. In Figure 5, corresponding to model 1 (no AVA effect), the picked amplitudes are flatter in the angle gather case. In Figure 6, corresponding to model 2 (decreasing amplitudes with increasing angles of incidence), the picked amplitudes follow the expected tendency more closely. The output in angle gather is a function

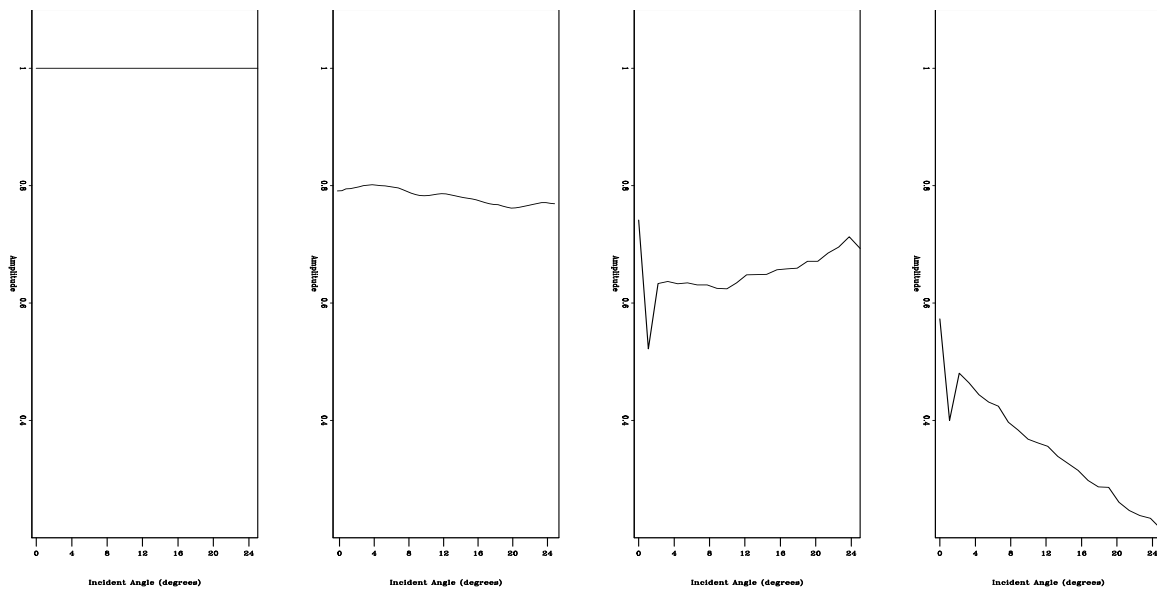


Figure 5: Picked amplitudes at the flat reflector for model 1: before migration (left), after migration and angle gather conversion (middle left), after migration (middle right) and conversion to angle domain, after migration/inversion and conversion to angle domain (right).
 cmora1-con_all [CR]

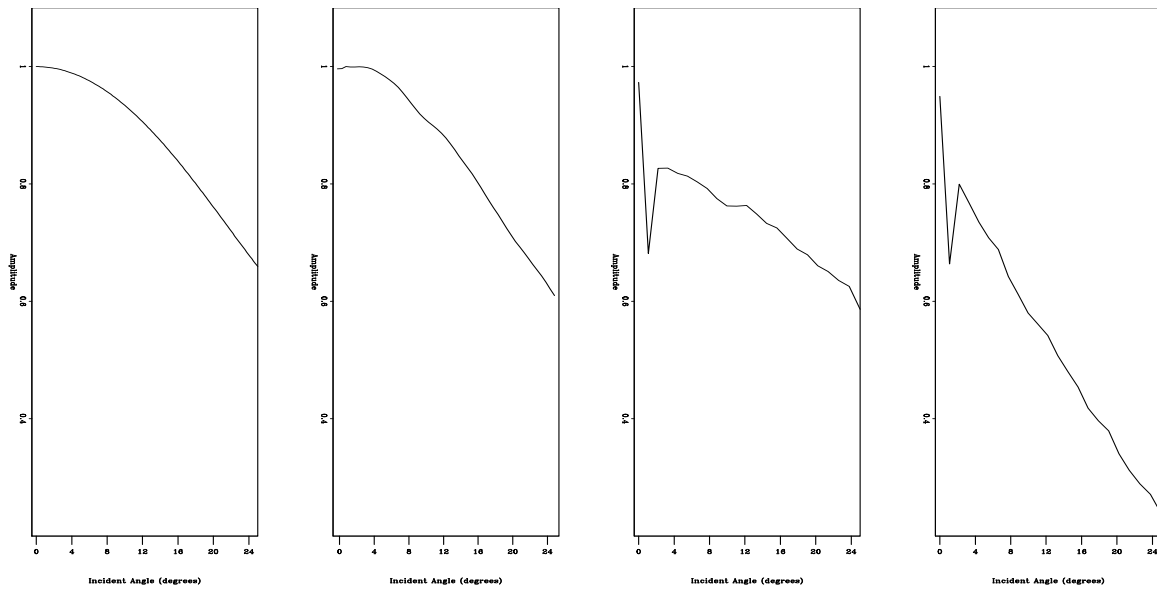


Figure 6: Picked amplitudes at the flat reflector for model 2: before migration (left), after migration and angle gather conversion (middle left), after migration (middle right) and conversion to angle domain, after migration/inversion and conversion to angle domain (right).
 cmora1-avo_all [CR]

of the reflection angle at the reflector, so no conversion is needed to do AVA analysis. Changing parameters (sampling, regularization, etc.) for the angle gather generation don't require re-migrating the data because migration and conversion to angle gather are separate processes. Results in the offset ray parameter domain could be improved if we use regularization in the inversion process (Prucha and Biondi, 2000); therefore, a next step should incorporate this approach.

CONCLUSION

I analyzed the amplitude behavior of angle gather and compared the resulting amplitudes from angle-domain common-image gathers with the amplitudes from offset-ray parameter images gathers in two models with and without AVA effect. Since results from angle gather are smoother and with a shape more similar to the theoretical tendency. I could observe that the angle gather method is not introducing amplitude distortions; therefore, this result gives us confidence about using this method in applications related to AVA analysis. Observed artifacts in offset ray parameter gather affect the picked amplitudes in the near and far offset. Typically, far offset amplitudes are not used in AVA analysis, but, in this case, near offset traces should be muted out in order to do AVA analysis. A next step should use regularization in the inversion process in order to improve the results in offset ray parameter domain.

ACKNOWLEDGMENTS

I would like to thank Paul Sava and Marie Prucha for providing the angle gather and the inversion codes I used in this paper, and for helping me with the use of these codes.

REFERENCES

Mavko, G., Mukerji, T., and Dvorkin, J., 1998, The rock physics handbook: Tools for seismic analysis in porous media: Cambridge University Press.

Ostrander, W. J., 1984, Plane-wave reflection coefficients for gas sands at nonnormal angles of incidence: *Geophysics*, **49**, no. 10, 1637–1648.

Prucha, M., and Biondi, B., 2000, Amplitudes and inversion in the reflection angle domain: *SEP-105*, 203–208.

Prucha, M. L., Biondi, B. L., and Symes, W. W., 1999, Angle-domain common image gathers by wave-equation migration: *SEP-100*, 101–112.

Prucha, M. L., Clapp, R. G., and Biondi, B., 2000, Seismic image regularization in the reflection angle domain: *SEP-103*, 109–119.

Sava, P., and Fomel, S., 2000, Angle-gathers by Fourier Transform: *SEP-103*, 119–130.

Swan, H. W., 1993, Properties of direct AVO hydrocarbon indicators *in* Castagna, J. P., and Backus, M. M., Eds., Offset dependent reflectivity — Theory and practice of AVO analysis:: Society of Exploration Geophysics, 78–92.

